J Solid State Electrochem (2011) 15:971–984
DOI 10.1007/s10008-010-1046-4

REVIEW

Sensing mechanism of non-equilibrium solid-electrolyte-based chemical sensors

Jeffrey W. Fergus

Received: 25 January 2010 / Revised: 3 March 2010 / Accepted: 5 March 2010 / Published online: 30 March 2010

Abstract Solid electrolytes can be used in several different types of chemical sensors. A common approach is to use the equilibrium potential generated across a solid electrolyte given by the Nernst equation as the sensing signal. However, in some cases, stable electrode materials are not available to establish equilibrium potentials, so non-equilibrium approaches are necessary. The sensing signal generated by such sensors is often described by the mixed potential theory, in which a pair of electrochemical reactions establishes a steady state at the electrode, such that the electrons produced by an oxidation reaction are consumed by a reduction reaction. The rates of both reactions depend on several factors, such as electron exchange, active area, and gas phase diffusion, so establishment of the steady-state potential is complex and alternative explanations have been proposed. This paper will review and discuss the mechanisms proposed to explain the sensor response of non-equilibrium-based electrochemical sensors.

Keywords Electrochemical sensors · Mixed potential · CO · NO_x

Introduction

Information on gas composition is important in many applications ranging from control of combustion processes to environmental monitoring. To meet these needs, gas sensors have been developed using a variety of different sensing approaches [1–9]. One approach is built on the pioneering work of Kiukkola and Wagner [10], who demonstrated the use of solid electrolytes for measurement of chemical potentials. Solid electrolytes are particularly useful in sensors for high-temperature applications and can be used in several different ways [11–18].

The most direct use of solid electrolytes in gas sensors is for measurement of a gas species corresponding to the ion that is mobile in the solid electrolyte. A common example of this is the use of an oxygen ion conductor, such as yttria-stabilized zirconia (YSZ), for the measurement of oxygen partial pressure, as in the exhaust gas from an internal combustion engine. Fortunately, however, detection is not limited to the mobile species because an auxiliary electrode can be added to provide sensitivity to another species by equilibrating between the desired target species and the ion that is mobile in the electrolyte. For example, the addition of sulfates or carbonates to various solid electrolytes (including oxygen-, sodium-, and lithium-ion conductors) can be used for the measurement of SO_2 and CO_2 gases [19]. However, this approach requires that the auxiliary electrode material be stable in the sensing environment, which limits the species that can be measured [20].

Although the Nernst potential on which potentiometric sensors are based is established by equilibration between the gas, electrolyte, and electrode, solid electrolytes can be used in non-equilibrium conditions, in which a steady state between electrochemical reactions establishes a potential that can be used as the sensor signal. The establishment of this potential can be described by the mixed potential theory that is commonly used to describe the corrosion of metals [21].

Mixed potential theory

The mixed potential sensing mechanism is based on the establishment of a steady state in which all the electrons

J. W. Fergus (✉)
Materials Research and Education Center, Auburn University,
275 Wilmore Laboratories,
Auburn, AL 36849, USA
e-mail: jwfergus@eng.auburn.edu

produced by an oxidation reaction are consumed by a reduction reaction [22–25]. This is essentially the same process that occurs in an equilibrium sensor except that for an equilibrium sensor the oxidation and reduction reactions are the same reaction but in opposite directions, whereas for a mixed potential sensor the oxidation and reduction reactions are for different species.

The establishment of a mixed potential is illustrated schematically in Fig. 1. The voltage in polarization plots is often plotted as the abscissa, which is appropriate for the results from a polarization experiment where the current is measured at a fixed voltage. However, current is used as the abscissa in Fig. 1 to reflect the idea that the currents associated with the rates of the two reactions establish the voltages. The upper two curves in Fig. 1a represent the oxidation

$$2O^{2-} \rightarrow O_2 + 4e^- \tag{1}$$

and reduction

$$O_2 + 4e^- \rightarrow 2O^{2-} \tag{2}$$

reactions for the equilibration between oxygen gas and oxygen ions in the electrolyte. The solid lines represent the net current in each direction, which approach zero as the voltages asymptotically approach the equilibrium redox potential. The linear portion of the curve represents the activation polarization, and the extrapolation of that linear curve to the equilibrium potential (indicated by a broken line) is the exchange current, which represents the rates of the forward and reverse reactions at equilibrium. The bottom portion of the figure shows a polarization curve for the oxidation of CO

$$2CO + 2O^{2-} \rightarrow 2CO_2 + 4e^- \tag{3}$$

and a small portion of the polarization curve for the reduction of CO_2

$$2CO_2 + 4e^- \rightarrow 2CO + 2O^{2-} \tag{4}$$

which establish a lower equilibrium potential than that established by oxygen gas.

The potentials for both reactions depend on the concentrations of the species. Using the reduction potentials, the concentration dependence of the potential (E) is given by

$$E = E_o - \frac{RT}{nF} \ln K, \tag{5}$$

where E_o is the standard reduction potential, R is the gas constant, T is temperature, F is Faraday's constant, and n is the number of electrons in the reduction reaction with equilibrium constant K. If CO and O_2 are both present at non-equilibrium conditions, such as those represented in Fig. 1a, the gases would react according to

$$2CO + O_2 \rightarrow 2O_2 \tag{6}$$

which would decrease the CO and O_2 concentrations and increase the CO_2 concentration. These changes in concentration would lead to an upward shift in the CO polarization

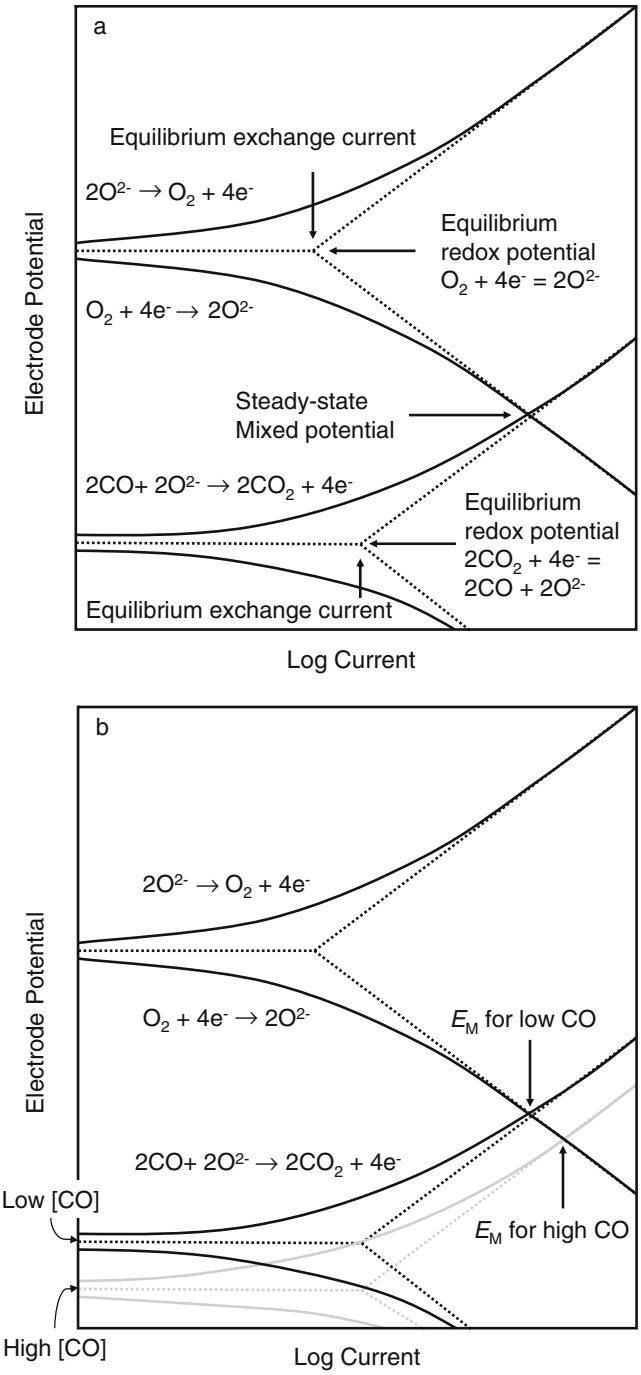

Fig. 1 Schematic CO and O_2 polarization curves. **a** Establishment of mixed potential. **b** Effect of changing CO concentration on mixed potential

curve (i.e., K for Reaction 4 decreases) and a downward shift in the O_2 polarization curve (i.e., K for Reaction 2 increases) until the equilibrium potentials become equal. In most practical applications of CO sensors, this does not occur (i.e., the gases do not equilibrate) so a mixed potential is established. The mixed potential is labeled in Fig. 1a and is the potential at which all the electrons from Reaction 3 are consumed by Reaction 2. The effect of the CO concentration on the mixed potential is shown in Fig. 1b. As indicated by Eq. 5, a decrease in the CO concentration will increase the reduction potential which will lead to an increase in the mixed potential (E_M).

Since only voltage differences rather than absolute voltages can be measured, a reference electrode is needed. The link to the reference electrode is provided by the solid electrolyte in which ions are mobile, so that the concentration of ionic defects (e.g., oxygen vacancies in YSZ) is the same throughout the bulk of the electrolyte and provides a link between the equilibria at the two electrode surfaces [11, 12]. In this paper, the voltages are reported with the reference electrode as the negative terminal. Although not always used, this convention is common, so if the signs of the electrodes were not specified in a paper from the literature, the reference electrode was assumed to be the negative terminal. The reference electrode can be based on an equilibrium potential, but in that case the reference and sensing electrodes must be separated by a gas-tight seal. However, if the reference potential is also based on a mixed potential, both electrodes can be exposed to the test gas, which, by eliminating the need for separate gas streams and a gas-tight seal between the two electrodes, simplifies the sensor design and thus reduces cost.

The differential response between the reference and sensing electrodes in a mixed potential sensor is achieved by selecting materials with different polarization behaviors. Figure 2 shows the polarization curves for the oxidation of CO (Reaction 3) and reduction of O_2 (Reaction 2) on two different electrodes: Reference electrode (Pt) and sensing electrode (SE). Linear polarization curves and equal exchange currents for the two electrodes are used in Fig. 2 to simplify the diagram and more clearly illustrate the trends in the mixed potentials established with different overpotentials and gas compositions. Platinum is typically used as the reference electrode, since it is a good catalyst, which results in a low overpotential (shallow slope). In Fig. 2a, the overpotentials for both the oxidation and reduction reactions on the sensing electrode are increased similarly (relative to Pt), in which case the mixed potential is not changed, so the potential difference between the reference and sensing electrodes is approximately zero. However, if the overpotentials for the two reactions change differently, the mixed potential is changed as shown in Fig. 2b and c. Figure 2b shows the case where the overpotential for the oxidation reaction on the sensing electrode increases more than the reduction reaction on the same electrode. In this case, the mixed potential on the sensing electrode is higher than that on the Pt reference

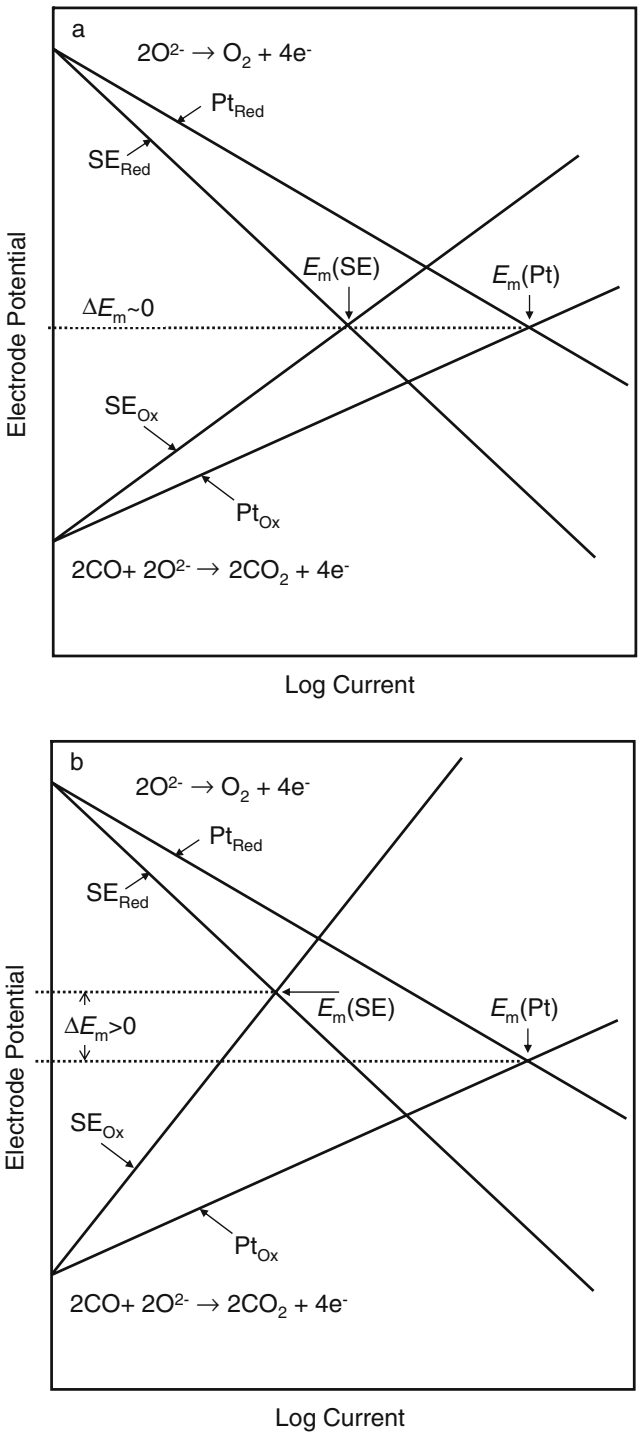

Fig. 2 Effect of electrode overpotential reducing gas (CO). **a** Oxidizing and reducing overpotentials affected similarly. **b** Oxidizing overpotential of sensing electrode increased more than reducing overpotential. **c** Reducing overpotential of sensing electrode increased more than oxidizing overpotential

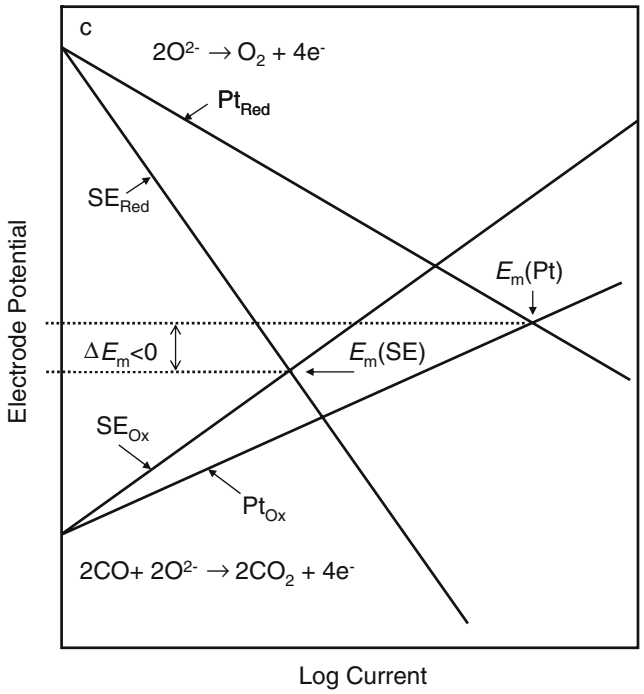

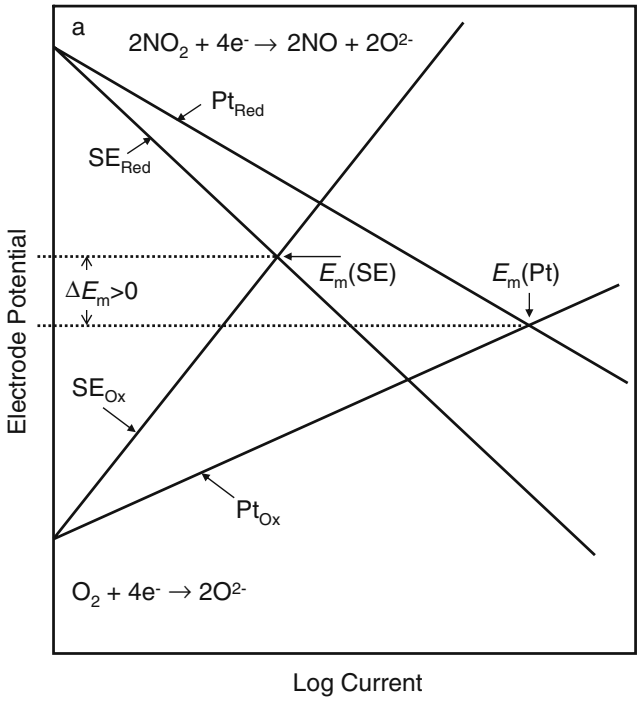

Fig. 2 (continued)

electrode, so a positive voltage will be generated. The reverse case, where the overpotential for the oxygen reduction reaction is increased more than the overpotential for the oxidation reaction, is shown in Fig. 2c. In this case, the potential at the sensing electrode is lower than that at the Pt reference electrode, so a negative voltage will be generated. The oxidation of CO is used as the example in Figs. 1 and 2, but the same mechanism would apply to any reducing gas (such as hydrocarbons) that would be oxidized by oxygen.

A mixed potential can also be generated with an oxidizing gas, such as NO_2, which is illustrated in Fig. 3. In this case, the relevant reactions are the oxidation of NO

$$2NO + 2O^{2-} \rightarrow 2NO_2 + 4e^- \quad (7)$$

and the reduction of NO_2

$$2NO_2 + 4e^- \rightarrow 2NO + 2O^{2-} \quad (8)$$

which are analogous to Reactions 3 and 4, but occur at a higher potential than the polarization curves for oxygen. The result of this is that the mixed potential is established between the oxidation of O^{2-} by Reaction 1 and the reduction of NO_2 by Reaction 8. Figure 3a shows that when the overpotential for the oxidizing reaction on the sensing electrode increases more than that for the reduction reaction, the mixed potential on the sensing electrode is higher than that on the reference Pt electrode, so the voltage difference is positive. As with the reducing gas shown in

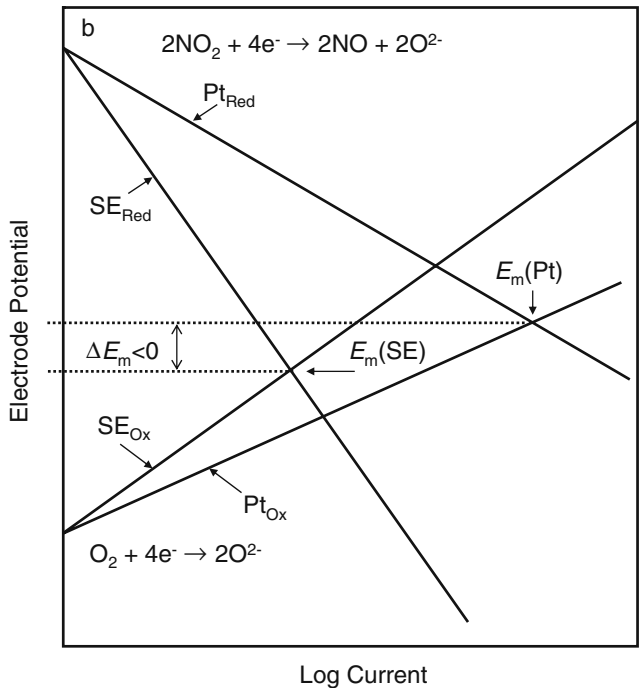

Fig. 3 Effect of electrode overpotential oxidizing gas (NO_2). **a** Oxidizing overpotential of sensing electrode increased more than reducing overpotential. **b** Reducing overpotential of sensing electrode increased more than oxidizing overpotential

Fig. 2, a change in which reaction overpotential is most affected by the electrode material reverses the sign of the voltage. Figure 3b shows that a negative voltage is generated when the overpotential for the reduction reaction on the sensing electrode is increased more than the

overpotential for the oxidation reaction. Thus, the sign of the response depends on the relative equilibrium voltages of the two reactions (i.e., oxidizing or reducing gas) and the overpotential that is most increased on the sensing electrode.

Figure 1b shows how the mixed potential on an electrode is changed by a change in gas composition. However, if the reference electrode is placed in the sample gas, which as noted above is a major advantage of mixed potential based sensors, the mixed potentials at both the sensing and reference electrodes will be affected. This is illustrated in Fig. 4, which includes the polarization curves for the oxidation of CO for two different CO concentrations. If the oxygen partial pressure is not changed, then the polarization curves for O_2 reduction will not change. Since both the reference and sensing potentials increase, the difference between the two mixed potentials is smaller than the difference between the two mixed potentials at the sensing electrodes for the two CO concentrations.

The electrochemical reaction rates can be limited by other factors, such as mass transport from the bulk gas to the electrode surface. In this case, the polarization curve is affected as illustrated in Fig. 5. In particular, at a certain overpotential, the current becomes limited by transport of gas to or from the electrode surface and does not increase with further increase in overpotential. Figure 5a shows a case in which the oxidation of CO reaches a plateau. Even though, in this example, the saturation current is the same for the two electrodes, the mixed potential is different because of the different overpotentials for the oxygen

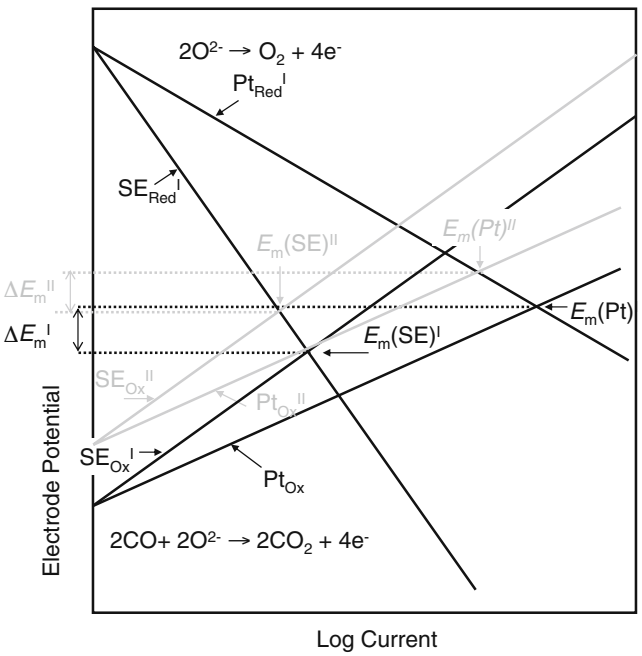

Fig. 4 Effect of gas concentration on mixed potential

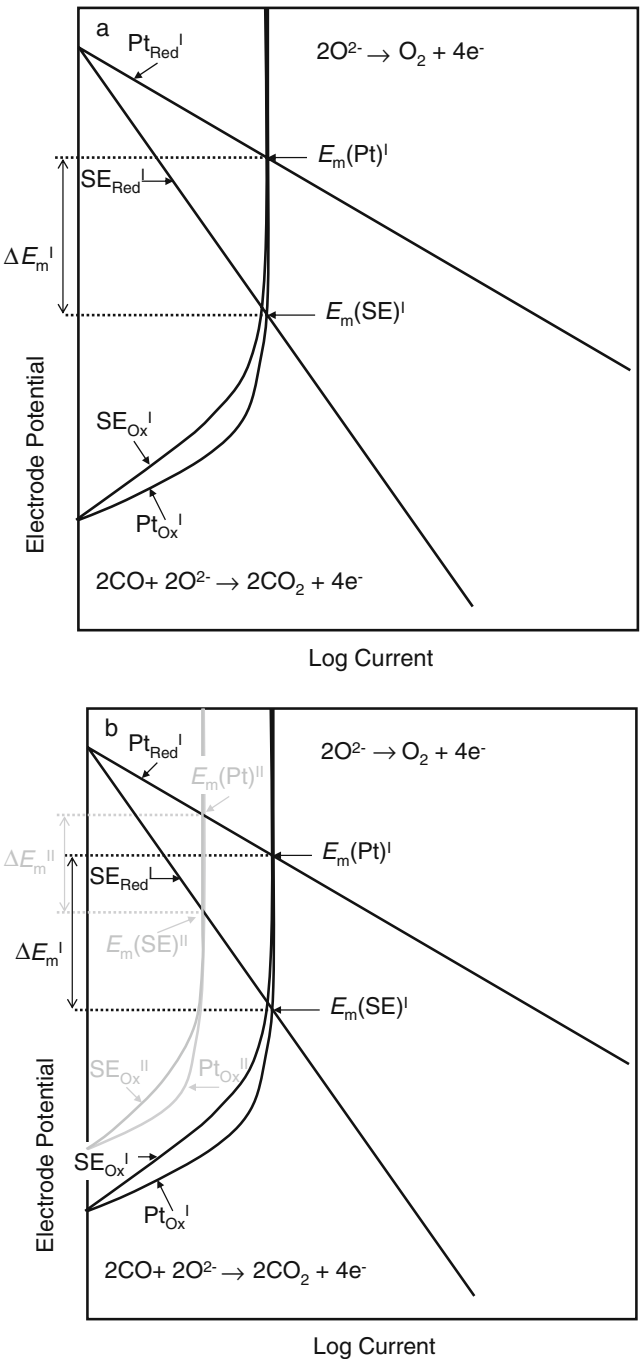

Fig. 5 Mixed potential with concentration overpotential. **a** Establishment of mixed potential. **b** Effect of changing CO concentration on mixed potential

reduction reaction. Figure 5b shows the effect of a change in CO concentration in the case of concentration polarization. In addition to the shift in the potential of the polarization curves (lower potential for higher CO concentration), as in Figs. 1b and 4, the limiting current can also change, since the maximum rate of supply of CO (in this example) will depend on the CO concentration in the bulk gas (larger current for higher CO concentration). This

change in the limiting current is the same as that used in amperometric sensors based on solid electrolytes. The result of these two factors is a larger (more negative) voltage with increasing CO concentration.

Non-equilibrium sensor performance

One of the simplest uses of a mixed potential is in a sensor with a Pt reference electrode and an Au sensing electrode for the measurement of CO. Figure 6 shows that the overpotential for the reduction of O_2 on a cerium gadolinium oxide (CGO) electrolyte with an Au electrode is higher than that with a Pt electrode [26]. The schematic in Fig. 2c indicates that an increase in the overpotential for oxygen reduction leads to a decrease in the mixed potential voltage, which would result in generation of negative voltage. A negative voltage has been observed for CO sensors with Pt and Au electrodes as shown in Fig. 7 [26–33]. The increased response with decreasing temperature of the sensors with CGO electrolytes shown in Fig. 7 correlates with the increasing overpotential with decreasing temperature shown in Fig. 6. In addition to the oxygen ion conducting electrolytes shown in Fig. 7 (e.g., samarium-doped ceria and YSZ), a sodium ion conducting electrolyte, beta alumina, has also been used in CO sensors with Au and Pt electrodes [34–36]. The sodium ion conducting electrolyte can be used for measurement of the mixed potential because the equilibrium between sodium oxide in the sodium beta alumina acts as an auxiliary electrode by providing equilibration between oxygen and sodium.

The addition of an oxide can inhibit microstructural changes in the Au electrode and thus improve sensor stability, particularly at high temperatures where sintering can occur [33]. Semiconducting oxides can also be used as the electrodes, some examples of which are shown in Fig. 8 [27, 37–43]. Several of these oxides generate negative voltages similar to Au electrodes, but there have been reports of positive voltages for $LaFeO_3$, $La_{0.8}Sr_{0.2}O_3$, and La_2CuO_4 electrodes [41–43]. Although the responses for sensors with $LaFeO_3$ or $La_{0.8}Sr_{0.2}O_3$ electrodes are relatively small, the response with a La_2CuO_4 electrode is large.

The largest response for a $LaCu_2O_4$ electrode was found at 300 °C, but this signal was not stable, in that the signals for increasing and decreasing gas concentration were different [43]; 300 °C was also the temperature at which the rate of CO desorption, according to temperature-programmed desorption (TPD) results, was maximum. As the temperature increased above 300 °C, the desorption and sensor signal decreased, so the response was attributed to adsorbed species. 300 °C was also the temperature above which the oxidation of CO occurred more slowly on La_2CuO_4 than on Pt according to temperature-programmed reaction (TPR) experiments. The slower oxidation on CO could lead to a mixed potential response with a positive sign if the slower rate were due to an increased overpotential for the oxidation of CO (see Fig. 2b) on La_2CuO_4.

The response of a sensor with Au and Nb_2O_5-covered Au has also been attributed to CO adsorption based on the absence of any catalysis of the CO oxidation for either electrode material as measured with TPR [44]. The response is attributed to a shift in the Fermi level of the semiconducting electrode due to adsorption on the electrode surface, but the mechanism by which this change relates to the electrochemical potentials in the solid electrolyte has not been described. Although both Au and Nb_2O_5-covered Au do not catalyze CO oxidation, there

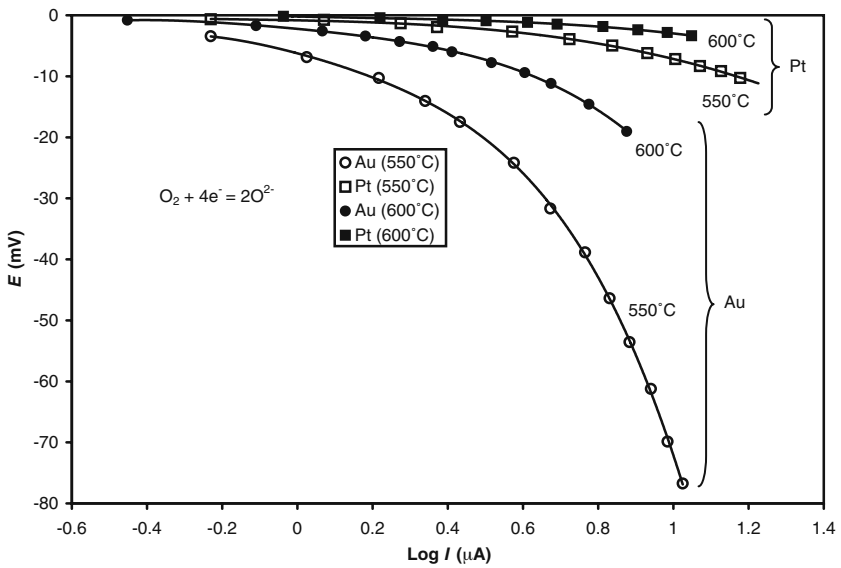

Fig. 6 O_2 reduction overpotential for Au and Pt electrodes on cerium gadolinium oxide (CGO) [26]

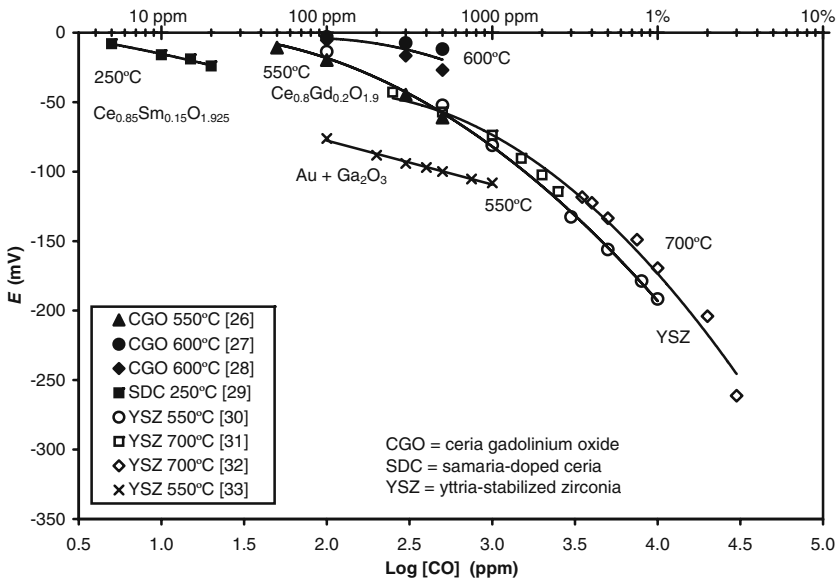

Fig. 7 Outputs for CO sensors with Pt and Au electrodes [26–33]

could still be a difference in their polarization behaviors, so a mixed potential response is possible. The changes in mixed potentials generally increase as the magnitude of the overpotential increases (i.e., steeper slopes in Figs. 1, 2, 3, 4, and 5), so even a relatively small difference in overpotentials may generate a measurable response.

As mentioned above, the mixed potential mechanism can be applied to other reducing gases, some examples of which are shown in Fig. 9 [32, 45–50]. Sensors with Pt and Au electrodes respond to hydrocarbon gases and the response increases with increasing molecule size (i.e., C_2H_4 to C_4H_8). A similar trend is observed using an oxide electrode (In_2O_3+MnO_2), but the response of the oxide electrode is larger. An oxide electrode (In_2O_3) has also been shown to respond to very small (sub parts per million) levels of C_3H_6. Figure 9 also shows that the sensor response can be changed by doping the electrolyte. In particular, the addition of titanium to the electrolyte leads to an increased response to C_3H_6, which illustrates the importance of the electrode–electrolyte interface in the polarization behavior. In addition to changes in the magnitude of the sensor response, changes in the sign can occur, as has been observed between CO and C_3H_6 for an Nb_2O_5 electrode [51]. The differences between the responses of different electrodes change with temperature, which provides an additional variable in the design of sensing systems for mixed gases, since multiple sensitivities can be obtained, even for a single sensing element, by varying the test

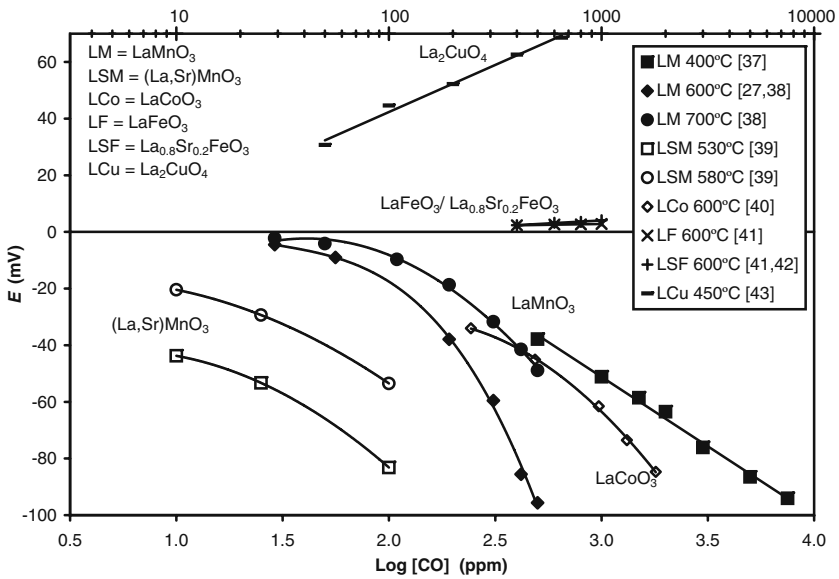

Fig. 8 Outputs for CO sensors with Pt and oxide electrodes [27, 37–43]

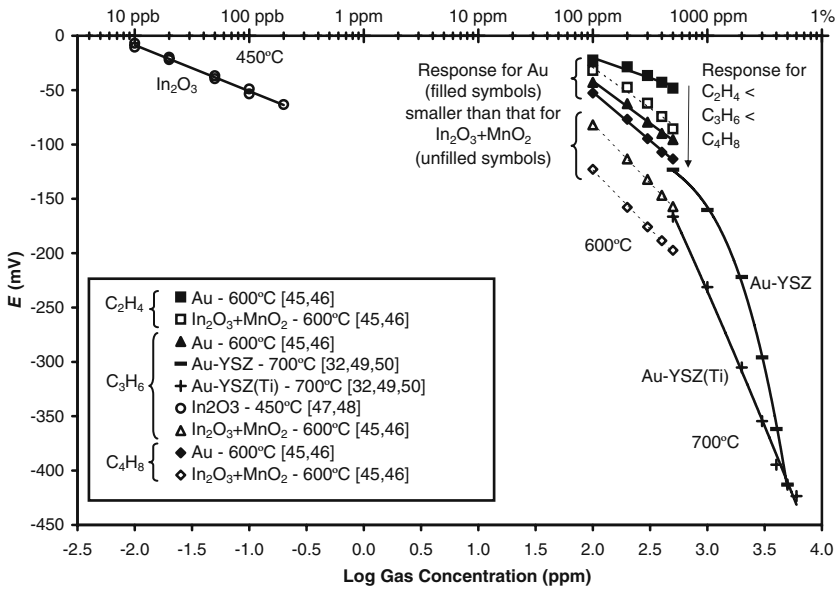

Fig. 9 Outputs for CO and hydrocarbon sensors with YSZ electrolytes [32, 45–50]

temperature. The ability to respond to multiple gases expands possible sensor applications and also creates challenges in obtaining satisfactory selectivity in multicomponent gases.

Another important application of non-equilibrium-based sensors is for the measurement of NO_x. Although equilibrium-based NO_x sensors have been reported, they have limited applicable ranges, so non-equilibrium-based sensors are more promising [52]. The equilibrium between the two common NO_x gases

$$2NO + O_2 \rightleftharpoons 2NO_2 \quad (9)$$

indicates that the NO_2 is favored at low temperatures and high oxygen partial pressures. In particular, the Gibbs energy for Reaction 9 is 0 at 491 and 235 °C for oxygen partial pressures of 10^5 and 10^3 Pa, respectively [53]. Since these conditions are similar to common sensing conditions, measurement of both gases by non-equilibrium sensors is possible.

The polarization behavior of NO_2 sensors was discussed above in Fig. 3, while that of NO would be analogous to CO described in Fig. 2. Although both sensors are based on the same reactions, the positions of the polarization curves relative to those of oxygen are different due to the different gas compositions (i.e., NO/NO_2 ratio). The responses of mixed potential gas sensors for NO and NO_2 are typically opposite in sign. The generally observed negative potential for NO and positive potential for NO_2 is consistent with the discussion above and indicates that the oxygen reaction controls the sensor response [54]. However, by applying a potential between the reference and sensing electrode, effectively shifting the relative positions of the polarization curves, the relative response to NO and NO_2 can be changed [55–58], which provides means for optimizing the sensor selectivity for a particular application.

The outputs of some NO_2 sensors with YSZ electrolytes and WO_3 electrodes are shown in Fig. 10 [41, 42, 59–67]. In one case [63], a tubular configuration, in which the electrodes were separated so the reference electrode could be exposed to a separate gas, was used to increase the sensor output. As discussed above, the potential of a reference electrode in the test gas, as in a planar sensor, is affected by changes in the test gas composition, so the sensor output may be smaller than that for a sensor with separated electrodes. In another case [65, 66], deposition of WO_3 on both the Pt and YSZ in a planar configuration was found to improve sensor response. The improvements were attributed to an interfacial layer inhibiting catalysis, which would increase the overpotential and thus increase the response as discussed above.

Another commonly used electrode material for NO_2 sensors is NiO, and the outputs of some sensors with NiO electrodes and YSZ electrolytes are shown in Fig. 11 [68–72]. As with the CGO-based CO sensors in Fig. 7, the magnitude of the response decreases with increasing temperature, which is expected for a sensor based on kinetic limitations, since those kinetic barriers are more easily overcome with the increased thermal energy at higher temperatures. The temperature dependence is also shown by the comparison in Fig. 12 of the sensitivities (millivolt per decade) of NO_2 sensors with WO_3 and NiO electrodes [41, 42, 59–63, 69–75].

According to Fig. 3a, a positive sensor response to an oxidizing gas, like NO_2, indicates an increased overpotential for the oxidation of O^{2-}. The anodic polarization curves for doped and undoped NiO electrodes in Fig. 13

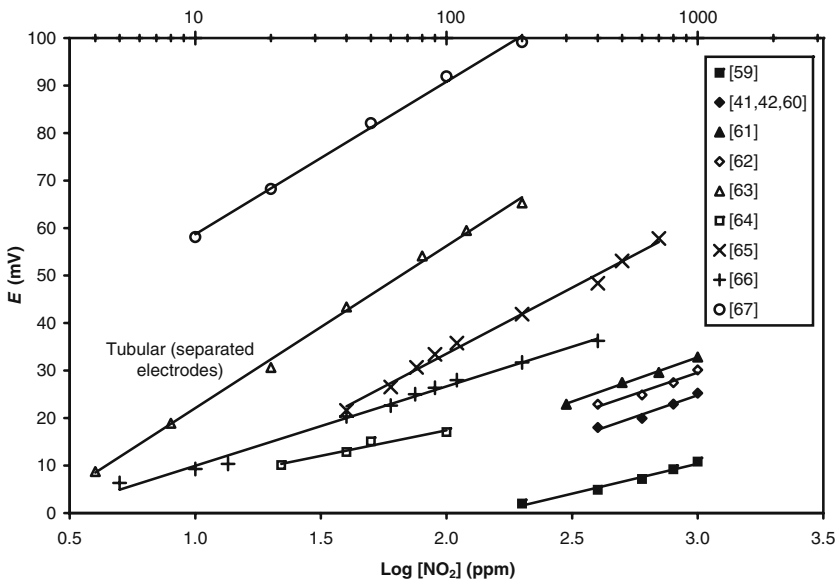

Fig. 10 Outputs for NO_2 sensors with Pt and WO_3 electrodes at 600 °C [41, 42, 59–67]

show that the overpotential for O^{2-} oxidation is increased with cobalt additions, but decreased with chromium additions [75, 76]. Figure 14 shows, consistent with Fig. 3a, that the increased overpotential (i.e., $Ni_{0.9}Co_{0.1}O$) generates a larger response, while the decreased overpotential (i.e., $Ni_{0.95}Cr_{0.03}O_{1-\delta}$) leads to a smaller response [71, 72, 74–76]. A similar increase in both polarization and sensor response has been observed with the addition of CuO to NiO [77].

There have been some reports of NO_2 sensors with responses that are opposite in sign to those of the WO_3- and NiO-based sensors discussed above. In particular, negative potentials have been observed for $La_{0.8}Sr_{0.2}FeO_3$ [41, 42, 60] and La_2CuO_4 [43] sensing electrodes with Pt reference electrodes and YSZ electrolytes. Because these are both p-type semiconductors, as compared to WO_3 which is an n-type semiconductor, the opposite signs of the responses have been related to the semiconductor nature of the electrode materials. However, NiO [78] as well as lanthanum chromite [79] and $(La,Sr)(Co,Fe)O_3$ [80] are also p-type semiconductors and generate a positive response when used in NO_2 sensors, as shown in Fig. 15 [41–43, 69, 81–83]. Although the p-type conduction does not alone explain the opposite sign, there is a difference in the response mechanism.

The response of sensors with La_2CuO_4 electrodes has been attributed to an absorption mechanism [43] based in part on infrared and X-ray photoelectron spectroscopy,

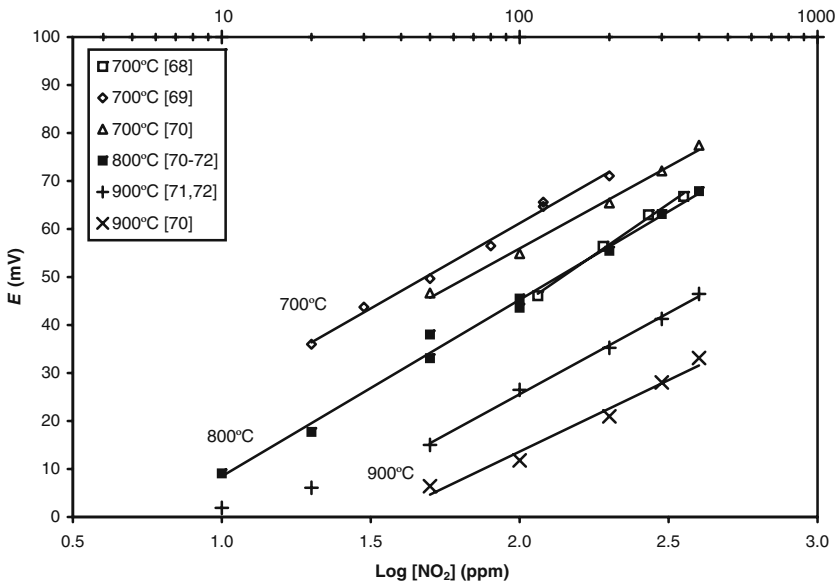

Fig. 11 Outputs for NO_2 sensors with Pt and NiO electrodes [68–72]

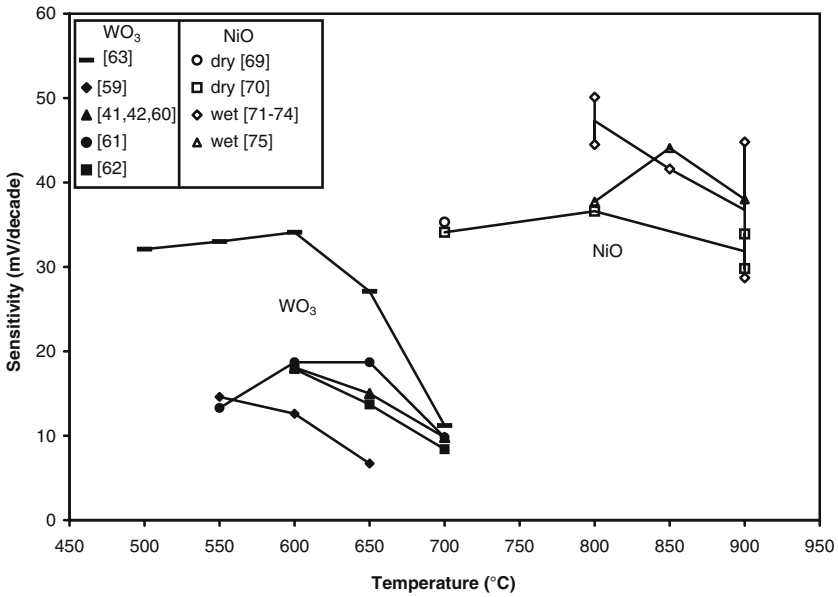

Fig. 12 Sensitivities of NO_2 sensors with Pt and WO_3 or NiO electrodes [41, 42, 59–63, 69–75]

which indicate that absorbed NO and NO_2 species lead to anionic species on the La_2CuO_4 surface [84]. The adsorbed species are suggested to lead to the formation of oxygen vacancies with electrons for NO adsorption and holes for NO_2 adsorption, which cause shifts in the Fermi level. The maximum response occurs at the same temperature at which NO_2 is reduced on both Pt and La_2CuO_4 surfaces as indicated by TPR results. The response decreases with increasing temperature, but a response is observed at temperatures at which TPD results indicate that most of the NO and NO_2 would have desorbed from the surface. There is a recent report of a NO_2 sensor based on the surface plasmon resonance of Au nanoparticles in a YSZ matrix [85], which suggests that NO_2 adsorption could affect the electronic state in the electrode. In addition, although generally considered to cancel out for symmetric Pt electrodes, the chemical potential of electrons in the electrode contributes to the measured potential of an electrochemical cell [11]. Changes in the Fermi potential could generate a sensor response, but for that response to be measured with a solid electrolyte, the change in potential needs to be related to the mobile ions in the solid electrolyte. This interaction would occur by redox reactions at the YSZ–La_2CuO_4 interface, which could be established by a mixed potential mechanism. According to TPR results, the reduction rates of NO_2 on Pt and La_2CuO_4 are similar [43]. However, the presence of adsorbed species or related inhibiting gas–solid interactions could affect the polarization behavior of the electrode, similar to the way that mass transport limitation can lead to concentration polarization,

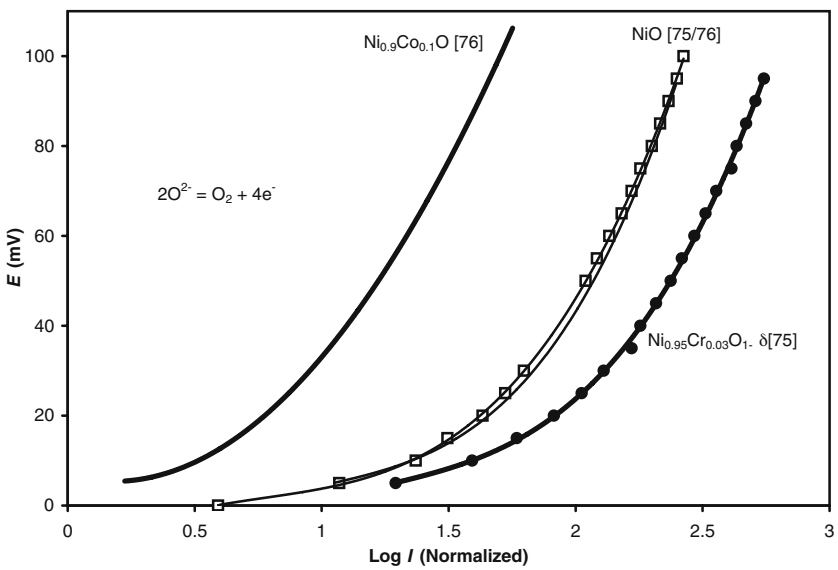

Fig. 13 O^{2-} oxidation overpotential for doped and undoped NiO electrodes at 800 °C [75, 76]. The NiO polarization curves were used to normalize the currents for direct comparison on a single graph

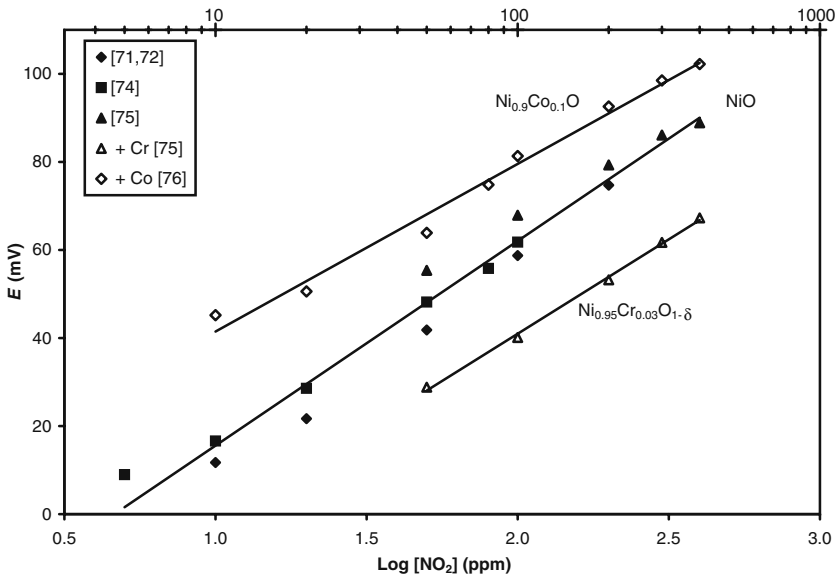

Fig. 14 Outputs of NO_2 sensors with Pt and doped/undoped NiO electrodes at 800 °C [71, 72, 74–76]

and establish a mixed potential on the electrode surface. The observed negative value of the response voltage would suggest that, according to Fig. 3b, whatever the inhibiting effect, the NO_2 reduction reaction is affected more than the O^{2-} oxidation reaction.

Electrode microstructure is particularly important in non-equilibrium-based sensors, since factors such as surface area and morphology affect reaction rates. For example, small grains [86] or small particles [87] have been shown to improve response. However, the effect of surface area in a non-equilibrium potentiometric sensor is different from that in many other sensors, such as semiconductor resistance-based sensors where high surface area is desired to enhance gas–solid interaction. For a mixed potential sensor, an increase in the electrode surface area would increase the rates of both reactions, so, at least under activation polarization, the mixed potential would not be changed. However, if the reaction was under concentration polarization, the rate would be limited by mass transport from the bulk gas to the electrode surface, which would not be affected by the increased surface area. Thus, a mixed potential between one reaction under activation polarization control and another under concentration polarization control can be affected by a change in the electrode surface area. For example, a NO_2 sensor based on two platinum electrodes with different surface morphologies responded to 40 ppm NO_2 and generated a signal of 80 mV at 800 ppm NO_2 [88].

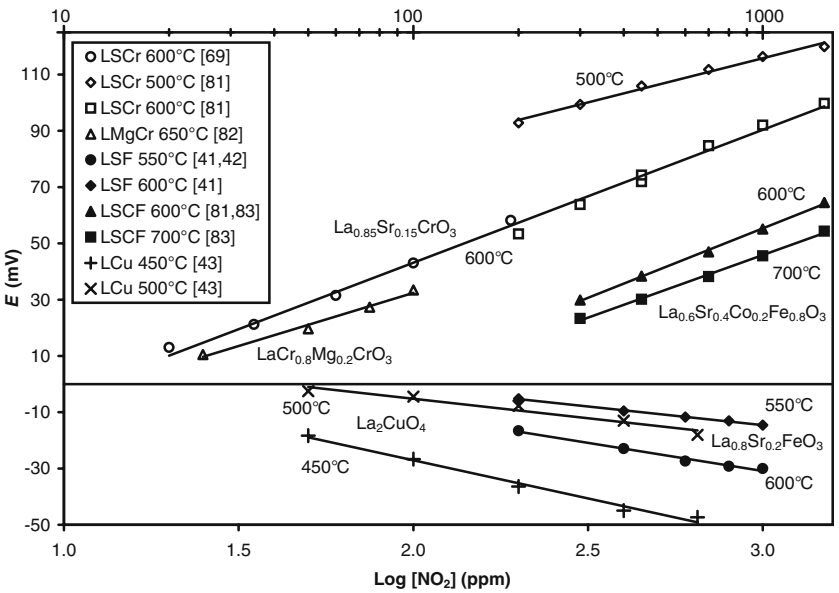

Fig. 15 Outputs for NO_2 sensors with Pt and oxide electrodes [41–43, 69, 81–83]

The usual approach in electrochemical devices is to have a dense electrolyte to separate the gases at the two electrodes with porous electrodes to increase the active surface area. However, in the case of mixed potential sensors, separation of the gases is not needed and high reaction rates are not desired for all reactions. Thus, sensors with porous electrolytes and dense $La_{0.8}Sr_{0.2}CrO_3$ [82, 89, 90] or (La,Sr)MnO_3 [39] electrodes have been reported. The advantage of the dense electrode is that heterogeneous catalysis by the electrode is minimized due to the low surface area, while the porous electrolyte allows for gas transport to the electrode–electrolyte interface.

Conclusions

Non-equilibrium-based electrochemical sensors provide the ability to sense gases, such as NO_x, CO, and hydrocarbons, that are difficult, if not impossible, to measure with equilibrium-based electrochemical sensors. The theory most often used to describe the sensing mechanism is the mixed potential theory, for which the sensor output is based on a steady state between four different electrochemical reactions. The sensor response is most often attributed to differences in the overpotential for oxygen reduction or oxygen-ion oxidation, but this explanation does not explain all observed sensor responses. Processes, such as adsorption, may inhibit the electrochemical reactions at the electrode surfaces, which may increase overpotentials and thus affect the electrode potentials. The multiple factors that can affect the outputs of non-equilibrium sensors provide opportunities for the development of new sensors, but also create challenges in understanding and controlling the sensor responses.

References

1. Azad A-M, Akbar S, Mhaisalkar SG, Birkefeld LD, Goto KS (1992) Solid-state gas sensors: a review. J Electrochem Soc 139:3690–3704
2. Yamazoe N, Miura N (1994) Environmental gas sensing. Sensors and Actuators B 20:95–102
3. Moos R (2005) A brief overview on automotive exhaust gas sensors based on electroceramics. Int J Appl Ceram Technol 2:401–413
4. Akbar S, Dutta P, Lee C (2006) High-temperature ceramic gas sensors: a review. Int J Appl Ceram Technol 3:302–311
5. Ivers-Tiffee E, Hardtl KH, Menesklou W, Riegel J (2001) Principles of solid state oxygen sensors for lean combustion gas control. Electrochim Acta 47:807–814
6. Lundström I (1996) Approaches and mechanisms to solid state based sensing. Sensors and Actuators B 35:11–19
7. Lee D-D, Lee D-S (2001) Environmental gas sensors. IEEE Sensors J 1:214–224
8. Moos R, Sahner K, Fleischer M, Guth U, Barsan N, Weimar U (2009) Solid state gas sensor research in Germany—a status report. Sensors 9:4323–4365
9. Guth U, Vonau W, Zosel J (2009) Recent developments in electrochemical sensor application and technology—a review. Meas Sci Technol 20:042002-1–042002-14
10. Kiukkola K, Wagner C (1957) Measurements of galvanic cells involving solid electrolytes. J Electrochem Soc 104:379–387
11. Weppner W (1987) Solid-state electrochemical gas sensors. Sensors and Actuators 12:107–119
12. Weppner W (1992) Advanced principles of sensors based on solid state ionics. Mater Sci Eng B15:48–55
13. Park CO, Akbar SA, Weppner W (2003) Ceramic electrolytes and electrochemical sensors. J Mater Sci 38:4639–4660
14. Zhuiykov S, Miura N (2005) Solid-state electrochemical gas sensors for emission control. In: Sorrell CC, Sugihara S, Nowotny J (eds) Materials for energy conversion devices. Woodhead, Cambridge, pp 303–335
15. Park CO, Fergus JW, Miura N, Park J, Choi A (2009) Solid-state electrochemical gas sensors. Ionics 15:261–284
16. Yamazoe N, Miura N (1998) Potentiometric gas sensors for oxidic gases. J Electroceramics 2:243–255
17. Pasierb P, Rekas M (2009) Solid-state potentiometric gas sensors—current status and future trends. J Solid State Electrochem 13:3–25
18. Möbius H-H, Hartung R (2010) Solid-state potentiometric gas sensors—a supplement. J Solid State Electrochem 14:669–673
19. Fergus JW (2008) Electrolyte and electrode materials for high temperature electrochemical CO_2 and SO_2 gas gensors. Sensors and Actuators B 134:1034–1041
20. Jacob KT, Swaminathan K, Sreedharan OM (1989) Stability constraints in the design of galvanic cells using composite electrolytes and auxiliary electrodes. Solid State Ionics 34:167–173
21. Jones DA (1996) Principles and prevention of corrosion, 2nd edn. Prentice-Hall, Upper Saddle
22. Miura N, Lu G, Yamazoe N (2000) Progress in mixed-potential type devices based on solid electrolyte for sensing redox gases. Solid State Ionics 136–137:533–542
23. Kotzeva VP, Kumar RV (1999) The response of yttria stabilized zirconia oxygen sensors to carbon monoxide gas. Ionics 5:220–226
24. Fergus JW (2007) Solid electrolyte based sensors for the measurement of CO and hydrocarbon gases. Sensors and Actuators B 122:683–693
25. Mari CM (2003) Non-Nernstian solid state gas sensors: operating principles and materials. Ionics 9:365–370
26. Mukundan R, Brosha EL, Brown DR, Garzon FH (2000) A mixed-potential sensor based on a $Ce_{0.8}Gd_{0.2}O_{1.9}$ electrolyte and platinum and gold electrodes. J Electrochem Soc 147:1583–1588
27. Garzon FH, Munkundan R, Brosha EL (2000) Solid-state mixed potential gas sensors: theory, experiments and challenges. Solid State Ionics 136–137:633–638
28. Mukundan R, Brosha EL, Brown DR, Garzon FH (1999) Ceria-electrolyte-based mixed potential sensors for the detection of hydrocarbons and carbon monoxide. Electrochem Solid-State Lett 2:412–414
29. Pijolat C, Tournier G, Viricelle JP (2009) Detection of CO in H_2-rich gases with a samarium doped ceria (SDC) sensor for fuel cell applications. Sensors and Actuators B 141:7–12
30. Vogel A, Baier G, Schüle V (1993) Non-Nernstian potentiometric zirconia sensors: screening of potential working electrode materials. Sensors and Actuators B 15–16:147–150
31. Butschbach P, Hammer F, Kohler H, Potreck A, Trautmann T (2009) Extensive reduction of toxic gas emissions of firewood-fueled low power fireplaces by improved in situ gas sensorics and catalytic treatment of exhaust gas. Sensors and Actuators B 137:32–41
32. Thiemann S, Hartung R, Wulff H, Klimke J, Möbius H-H, Guth U, Schönauer U (1996) Modified Au-YSZ electrodes—prepara-

tion, characterization and electrode behaviour at higher temperatures. Solid State Ionics 86–88:873–876
33. Shuk P, Bailey E, Zosel J, Guth U (2009) New advanced in situ carbon monoxide sensor for the process application. Ionics 15:131–138
34. Lalauze R, Visconte E, Montanaro L, Pijolat C (1993) A new type of mixed potential sensor using a thick film of beta alumina. Sensors and Actuators B 13–14:241–243
35. Guillet N, Lalauze R, Pijolat C (2004) Oxygen and carbon monoxide role on the electrical response of a non-Nernstian potentiometric gas sensor; proposition of a model. Sensors and Actuators B 98:130–139
36. Guillet N, Lalauze R, Viricelle JP, Pijolat C, Montanaro L (2002) Development of a gas sensor by thick film technology for automotive applications: choice of materials—realization of a prototype. Mater Sci Eng C 21:97–103
37. Sorita R, Kawano T (1997) A highly selective CO sensor using $LaMnO_3$ electrode-attached zirconia galvanic cell. Sensors and Actuators B 40:29–32
38. Brosha EL, Mukundan R, Brown DR, Garzon FH (2002) Mixed potential sensors using lanthanum manganate and terbium yttrium zirconium oxide electrodes. Sensors and Actuators B 87:47–57
39. Morata A, Viricelle JP, Tarancón A, Dezanneau G, Pijolat C, Peiro F, Morante JR (2008) Development and characterisation of a screen-printed mixed potential gas sensor. Sensors and Actuators B 130:561–566
40. Brosha EL, Mukundan R, Brown DR, Garzon FH, Visser JH, Zanini M, Zhou Z, Logothetis EM (2000) CO/HC sensors based on thin films of $LaCoO_3$ and $La_{0.8}Sr_{0.2}CoO_{3-\delta}$ metal oxides. Sensors and Actuators B 69:171–182
41. Di Bartolomeo E, Kaabbuathong N, Grilli ML, Traversa E (2004) Planar electrochemical sensors based on tape-cast YSZ layers and oxide electrodes. Solid State Ionics 171:173–181
42. Di Bartolomeo E, Grilli ML, Traversa E (2004) Sensing mechanism of potentiometric gas sensors based on stabilized zirconia with oxide electrodes. J Electrochem Soc 151:H133–H139
43. Yoo J, Chatterjee S, Van Assche FM, Wachsman ED (2007) Influence of adsorption and catalytic reaction on sensing properties of a potentiometric La_2CuO_4/YSZ/Pt sensor. J Electrochem Soc 154:J190–J195
44. Chevallier L, Di Bartolomeo E, Grilli ML, Mainas M, White B, Wachsman ED, Traversa E (2008) Non-Nernstian planar sensors based on YSZ with a Nb_2O_5 electrode. Sensors and Actuators B B129:591–598
45. Hibino T, Tanimoto S, Kakimoto S, Sano M (1999) High-temperature hydrocarbon sensors based on a stabilized zirconia electrolyte and metal oxide electrodes. Electrochem Solid-State Lett 2:651–653
46. Hibino T, Hashimoto A, Kakimoto S, Sano M (2001) Zirconia-based potentiometric sensors using metal oxide electrodes for detection of hydrocarbons. J Electrochem Soc 148:H1–H5
47. Miura N, Mori S, Wama R, Elumalai P, Plashnitsa VV, Utiyama M (2008) Mixed-potential-type YSZ-based sensor capable of detecting propene at several tens ppb level. Electrochem Solid-State Lett 11:J69–J71
48. Wama R, Plashnitsa VV, Elumalai P, Kawaguchi T, Fujio Y, Masahiro MN (2009) Improvement in propene sensing characteristics by the use of additives to In_2O_3 sensing electrode of mixed-potential-type zirconia sensor. J Electrochem Soc 156:J102–J107
49. Somov S, Reinhardt G, Guth U, Göpel W (1996) Gas analysis with arrays of solid state electrochemical sensors: implications to monitor HCs and NO_x in exhausts. Sensors and Actuators B 35–36:409–418
50. Göpel W, Reinhardt G, Rösch M (2000) Trends in the development of solid state amperometric and potentiometric high temperature sensors. Solid State Ionics 136–137:519–531
51. Chevallier L, Di Bartolomeo E, Grilli ML, Traversa E (2008) High temperature detection of CO/HCs gases by non-Nernstian planar sensors using Nb_2O_5 electrode. Sensors and Actuators B 130:514–519
52. Fergus JW (2007) Materials for high temperature electrochemical NO_x gas sensors. Sensors and Actuators B 121:652–663
53. Chase MW Jr (1998) NIST-JANAF thermochemical tables. J Phys Chem Ref Data, Monograph No. 9, 4th edn
54. Park CO, Miura N (2006) Absolute potential analysis of the mixed potential occurring at the oxide/YSZ electrode at high temperature in NO_x-containing air. Sensors and Actuators B 113:316–319
55. Zhuiykov S, Nakano T, Kunimoto A, Yamazoe N, Miura N (2007) Potentiometric NO_x sensor based on stabilized zirconia and $NiCr_2O_4$ sensing electrode operating at high temperatures. Electrochem Comm 3:97–101
56. West D, Montgomery F, Armstrong T (2005) DC electrical-biased, all-oxide NO_x sensing elements for use at 873 K. Ceram Eng Sci Proc 26:49–56
57. West DL, Montgomery FC, Armstrong TR (2006) Total NO*x*' sensing elements with compositionally identical oxide electrodes. J Electrochem Soc 153:H23–H28
58. West DL, Montgomery FC, Armstrong TR (2005) Electrically biased NO_x sensing elements with coplanar electrodes. J Electrochem Soc 152:H74–H79
59. Di Bartolomeo E, Grilli ML (2005) YSZ-based electrochemical sensors: from materials preparation to testing in the exhausts of an engine bench test. J Eur Ceram Soc 25:2959–2964
60. Di Bartolomeo E, Kaabbuathong N, D'Epifanio A, Grilli ML, Traversa E, Aono H, Sadaoka Y (2004) Nano-structures perovskite oxide electrodes for planar electrochemical sensors using tape casted YSZ layer. J Eur Ceram Soc 24:1187–1190
61. Dutta A, Kaabbuathong N, Grilli ML, Di Bartolomeo E, Traversa E (2003) Study of YSZ-based electrochemical sensors with WO_3 electrodes in NO_2 and CO environments. J Electrochem Soc 150: H33–H37
62. Grilli ML, Chevallier L, Di Vona ML, Licoccia S, Di Bartolomeo E (2005) Planar electrochemical sensors based on YSZ with WO_3 electrode prepared by different chemical routes. Sensors and Actuators B 111–112:91–95
63. Lu G, Miura N, Yamazoe N (2000) Stabilized zirconia-based sensors using WO_3 electrode for detection of NO or NO_2. Sensors and Actuators B 65:125–127
64. Di Bartolomeo E, Grilli ML, Yoon JW, Traversa E (2004) Zirconia-based electrochemical NO_x sensors with semiconducting oxide electrodes. J Am Ceram Soc 87:1883–1889
65. Yang J-C, Dutta PK (2009) Solution-based synthesis of efficient WO_3 sensing electrodes for high temperature potentiometric NO_x sensors. Sensors and Actuators B 136:523–529
66. Yang J-C, Spirig JV, Karweik D, Routbort JL, Singh D, Dutta PK (2008) Compact electrochemical bifunctional NO_x/O_2 sensor with metal/metal oxide internal reference electrode for high temperature applications. Sensors and Actuators B 131:448–454
67. Yoo J, Van Assche FM, Wachsman ED (2006) Temperature-programmed reaction and desorption of the sensor elements of a WO_3/YSZ/Pt potentiometric sensors. J Electrochem Soc 153:H115–H121
68. Park J, Yoon BY, Park CO, Lee W-J, Lee CB (2009) Sensing behavior and mechanism of mixed potential NO_x sensors using NiO, NiO(+YSZ) and CuO oxide electrodes. Sensors and Actuators B 135:516–523
69. West DL, Montgomery FC, Armstrong TR (2005) NO-selective NO_x sensing elements for combustion exhausts. Sensors and Actuators B 111–112:84–90

70. Elumalai P, Wang J, Zhuiykov S, Terada D, Hasei M, Miura N (2005) Sensing characteristics of YSZ-based mixed-potential-type planar NO_x sensors using NiO sensing electrodes sintered at different temperatures. J Electrochem Soc 152:H95–H101
71. Miura N, Wang J, Nakatou M, Elumalai P, Hasei M (2005) NO_x sensing characteristics of mixed-potential-type zirconia sensor using NiO sensing electrode at high temperatures. Electrochem Solid-State Lett 8:H9–H11
72. Miura N, Wang J, Nakatou M, Elumalai P, Zhuiykov S, Hasei M (2006) High-temperature operating characteristics of mixed-potential-type NO_2 sensor based on stabilized-zirconia tube and NiO sensing electrode. Sensors and Actuators B 114:903–909
73. Elumalai P, Miura N (2005) Performances of planar NO_2 sensor using stabilized zirconia and NiO sensing electrode at high temperature. Solid State Ionics 176:2517–2522
74. Wang J, Elumalai P, Terada D, Hasei M, Miura N (2006) Mixed-potential-type zirconia-based NO_x sensor using Rh-loaded NiO sensing electrode operating at high temperatures. Solid State Ionics 177:2305–2311
75. Elumalai P, Zosel J, Guth U, Miura N (2009) NO_2 sensing properties of YSZ-based sensor using NiO and Cr-doped NiO sensing electrodes at high temperature. Ionics 15:405–411
76. Elumalai P, Plashnitsa V, Fujio Y, Miura N (2009) Tunable NO_2-sensing characteristics of YSZ-based mixed-potential-type sensor using $Ni_{1-x}Co_xO$-sensing electrode. J Electrochem Soc 156:J288–J293
77. Plashnitsa VV, Ueda T, Miura N (2006) Improvement of NO_2 sensing performances by an additional second component to the nano-structured NiO sensing electrode of a YSZ-based mixed-potential-type sensor. Int J Appl Ceram Technol 3:127–133
78. Kofstad P (1983) Nonstoichiometry, diffusion, and electrical conductivity in binary metal oxides. Robert E. Krieger, Malabar
79. Akashi T, Maruyama T, Goto T (2003) Transport of lanthanum ion and hole in $LaCrO_3$ determined by electrical conductivity measurements. Solid State Ionics 64:177–183
80. Tai L-W, Nasrallah MM, Anderson HU, Sparlin DM, Sehlin SR (1995) Structure and electrical properties of $La_{1-x}Sr_xCo_{1-y}Fe_yO_3$ materials. Part 2. The system $La_{1-x}Sr_xCo_{0.2}Fe_{0.8}O_3$. Solid State Ionics 76:273–283
81. West DL, Montgomery FC, Armstrong TR (2005) Use of $La_{0.85}Sr_{0.15}CrO_3$ in high-temperature NO_x sensing elements. Sensors and Actuators B 106:758–765
82. Brosha EL, Mukundan R, Lujan R, Garzon FH (2006) Mixed potential NO_x sensors using thin film electrodes and electrolytes for stationary reciprocating engine type applications. Sensors and Actuators 119:398–408
83. West DL, Montgomery FC, Armstrong TR (2004) Electrode materials for mixed-potential NO_x sensors. Ceram Eng Sci Proc 25:493–498
84. Van Assche FM IV, Nino JC, Wachsman ED (2008) Infrared and x-ray photoemission spectroscopy of absorbates on La_2CuO_4 to determine potentiometric NO_x sensor response mechanism. J Electrochem Soc 155:J198–J204
85. Rogers PH, Sirinakis G, Carpenter MA (2008) Plasmonic-based detection of NO_2 in a harsh environment. J Phys Chem C 112:8784–8790
86. White B, Chatterjee S, Macam E, Wachsman E (2008) Effect of electrode microstructure on the sensitivity and response time of potentiometric NO_x sensors. J Am Ceram Soc 91:2024–2031
87. Plashnitsa VV, Elumalai P, Fujio Y, Miura N (2009) Zirconia-based electrochemical gas sensors using nano-structured sensing materials aiming at detection of automotive exhausts. Electrochimica Acta 54:6099–6106
88. Yang J-C, Dutta PK (2010) High temperature potentiometric NO_2 sensor with asymmetric sensing and reference Pt electrodes. Sensors and Actuators B 143:459–463
89. Sekhar PK, Brosha EL, Mukundan R, Li W, Nelson MA, Palanisamy P, Garzon FH (2010) Application of commercial automotive sensor manufacturing methods for NO_x/NH_3 mixed potential sensors for on-board emissions control. Sensors and Actuators B 144:112–119
90. Mukundan R, Teranishi K, Brosha EL, Garzon FH (2007) Nitrogen oxide sensors based on yttria-stabilized zirconia electrolyte and oxide electrodes. Electrochem Solid-State Lett 10:J26–J29